The Impact of Mineral Deposition by Carbonation and Dissolution on Leaching of Constituents from a Cement Mortar - 10312

J. Arnold[*], J.C.L. Meeussen[**], A. Garrabrants[*], H. van der Sloot[**], and D. S. Kosson[*]
[*] Vanderbilt University, Department of Civil and Environmental Engineering, Nashville, Tennessee, USA
[**] Energy Research Centre of the Netherlands, Environmental Risk Assessment Biomass, Coal & Environmental Research, Petten, NL

ABSTRACT

Cementitious materials are widely utilized in waste containment and stabilization applications due in part to the rather tortuous nature of their interconnected pore networks, thereby providing a physical barrier to contaminant release. Modeling the performance of cementitious materials in the natural environment is convoluted by a multitude of processes that may induce changes in the solid matrix, thereby altering the intrinsic tortuosity of the pore space. Leaching of calcium phases, precipitation of carbonates, ettringite, thaumasite, and brucite, among others, are chemical processes known to change pore structure of cementitious materials. Macroscopic models are ill-suited for describing these pore-changing phenomena as they typically occur in reaction fronts resulting localized filling or opening of pore space. The geochemical speciation and mass transport solver ORCHESTRA has been implemented to model porosity change of a blended cement mortar as a consequence of mineral dissolution and calcite precipitation. Simulation of a diffusion-controlled leaching test with deionized water was performed to demonstrate the effects of primary constituent leaching on major constituent leaching. Additionally, the response of a mortar stored in a 5% carbon dioxide atmosphere at 65% RH was simulated for 168 weeks.

INTRODUCTION

The rate at which a given chemical species is transported within a porous material is fundamentally dependent upon the morphological characteristics of the interconnected pore space. Cementitious materials are generally characterized by highly tortuous pore networks such that the rates of ingress and egress of chemical species is quite slow. In ordinary Portland cement (OPC) as well as blends of OPC, fly ash (FA), and blast furnace slag (BFS), the morphology of the pore space is determined from the hydration of primary solid phases, wherein water may be incorporated into the lattice structure of, primarily, the amorphous phase calcium silicate hydrate (C-S-H). Modeling the performance of these materials in the natural environment is convoluted by a multitude of processes that may induce changes in the solid matrix, thereby altering the intrinsic tortuosity of the pore space. Leaching of calcium phases, precipitation of carbonates, ettringite, thaumasite, and brucite, among others, are chemical processes known to alter the pore structure of cementitious materials. Macroscopic models are ill-suited for describing these pore-changing phenomena as they typically occur in reaction fronts resulting localized filling or opening of pore space.

MATERIALS AND METHODS
A blended cementitious mortar containing OPC, FA, BFS, and quartz sand was chosen for this study. The proportions of each material are within the range expected for many engineering applications and are shown in Table I.

The chemical characteristics of the mortar were determined through a pH dependent leaching test wherein crushed sample is leached with solutions of varied acidity and alkalinity such that the leachates' pH span from 2 to 12 after 48 hours of exposure [1]. In this manner, the available fractions of primary constituents (that which is leachable under environmental conditions within human timescales) were determined for use as a model input.

MODEL FORMULATION

The one-dimensional diffusion reaction equation for a species diffusing into a porous medium in the -direction is given by

$$ \frac{}{} = , \frac{}{} + \qquad\qquad \text{(Eq. 1)} $$

where is the connected porosity of the specimen[m^3 connected pore volume / m^3 sample volume], is the concentration of species [mol/L pore solution], , [m^2/s] is the effective diffusivity of species . and is a reaction term reflecting the dissolution or precipitation of each solid matrix phase [mol/m^3·s]. ORCHESTRA is a software code that solves the diffusion reaction equation for an arbitrary set of chemical species by decoupling the partial differential equation (1) into an alternating sequence of chemical equilibrium and mass transfer calculations Chemical equilibrium is solved according to the laws of mass action, mass conservation and charge conservation for each point, or node, in the discretization of [m]. Equilibrium constants for each the solid species present in the current material are taken from the current literature [2].
   The present research incorporates into ORCHESTRA the ability to quantify change in the interconnected porosity Δ at each node as a result of precipitation and dissolution reactions via

$$, - , \times , = - \frac{\overline{\quad}}{,\qquad,} = -\Delta \qquad\qquad \text{(Eq. 2)} $$

where , and , [mol] are the masses of solid phase at times and 0, respectively, , [m^3 / mol] is the molar volume of the solid phase , , and , [m^3] are the pore volumes at times and 0, respectively, and [m^3] is the total volume of the node.

Table I: Mix Design Proportions

Mix Component	Mass Percent
OPC	5.88
FA	6.62
BFS	13.48
Quartz sand	62.25
Water (w/b = 0.38)	11.76

Table II: Initial Model Parameter Values

Parameter	Value
	0.08
	150
	0.60
	10^{-9} m^2/s
	10^{-7} m^2/s

The impact of porosity change on both ionic diffusivity and gas diffusivity is examined by defining the effective diffusivity constant $_,$ [m^2/s] as

$$_, = \frac{}{}$$ (Eq. 3)

where tortuosity [m diffusion path length / m Euclidean distance] accounts for the non-linear mean diffusion path within the pore space due to physical interactions with the pore walls. It should be noted that since the impact of ionic strength on rate of diffusion is not explicitly considered herein, ion-ion interactions are also reflected in the tortuosity term [3].

A number of relationships for $_,$ as a function of porosity have been presented in the literature [4-7]. A form of this relation that has been employed for both porosity filling and opening has been adopted for this work and is given as [7]

$$_, = \frac{}{} \exp\left[\frac{4.3}{}(-)\right]$$ (Eq. 4)

where is the volumetric paste fraction of the material [m^3 paste / m^3 total], is the connected porosity at time , and is the initial connected porosity of the material. Initial simulation parameter values are shown in Table II.

The first mass transport scenario simulated herein is exposure to deionized water at a liquid volume to specimen surface area ratio of 10 [mL / cm^2]. Leaching solution was renewed at one-week intervals for a duration of 168 days. The second scenario simulated exposure of a sample to a constant ambient atmosphere of 5% by volume CO_2 (g) for a period of 168 days. Specimen saturation with pore solution was maintained at 75 %. The effective diffusivity of the gas phase was assumed to be 4.4 (10^{-8}) [m^2/s] to account for the effect of saturation on the gas phase tortuosity.

RESULTS

Profiles of mineral composition as a function of depth are shown in Fig. **1** for the deionized water leaching simulation. The depth of mineral dissolution, or depletion depth, is 9 mm at 6 and 12 mm at 24 weeks, and the total mineral volume at 24 weeks is approximately half that present at 6 weeks. The decrease in mineral volume is primarily due to the dissolution of Portlandite, which accounts for more than half of the initial mineral volume. The increase in ettringite volume through DI water leaching can be attributed to the overall decrease in alkalinity within the reaction front.

Fig. **2** illustrates the mineral volume change induced by the ingress of CO_2(g). After 6 weeks of exposure, the most dramatic net solid volume change occurs at a depth of 9 mm and is primarily due to the precipitation of tricarboaluminate, calcite, and ettringite. At 24 weeks of exposure, the greatest net volume change remains 9 mm from the external surface, but the proportion of ettringite has increased while tricarboaluminate has been almost completely dissolved. At a depth greater than 9 mm, however, tricarboaluminate persists and accounts for the net increase in solid volume.

It should be noted that the penetration depth of the carbon dioxide front is 90 mm after 24 weeks, as evidenced by the slight dissolution of portlandite observed in Fig. **2** (b) and the corresponding porosity increase in Figure 3 (b). In this regime, the pH of the pore solution is slightly depressed

by dissolved carbonate but remains undersaturated in carbonate such that calcite and tricarboaluminate do not precipitate.
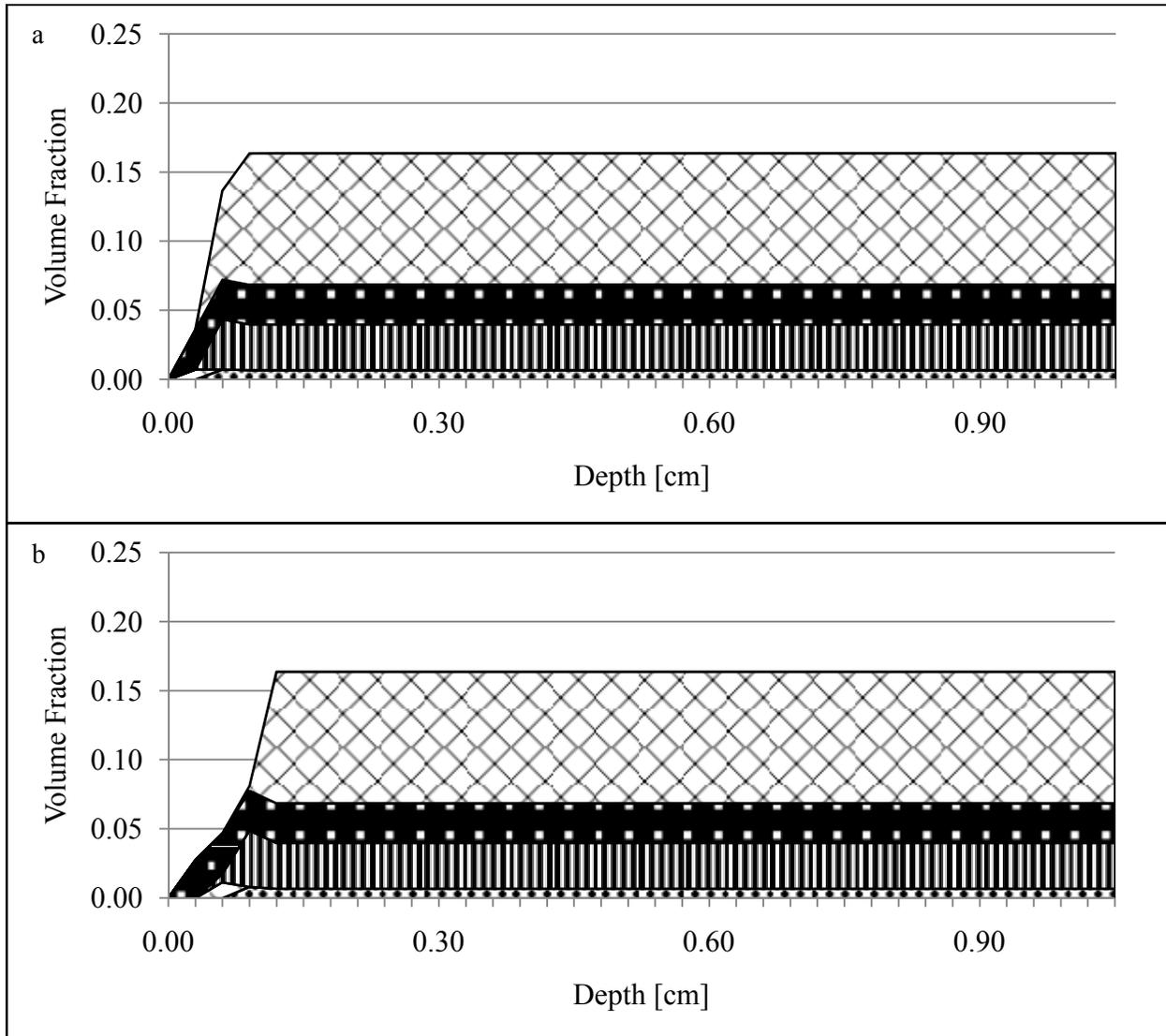

Fig. 1: Contributions of individual solid species to total mineral volume at a) 6 weeks and b) 24 weeks of deionized water leaching with weekly renewal of the leaching solution. The solid phases present are: portlandite (hatch), calcite (white squares), ettringite (vertical lines), C-S-H (black circles).
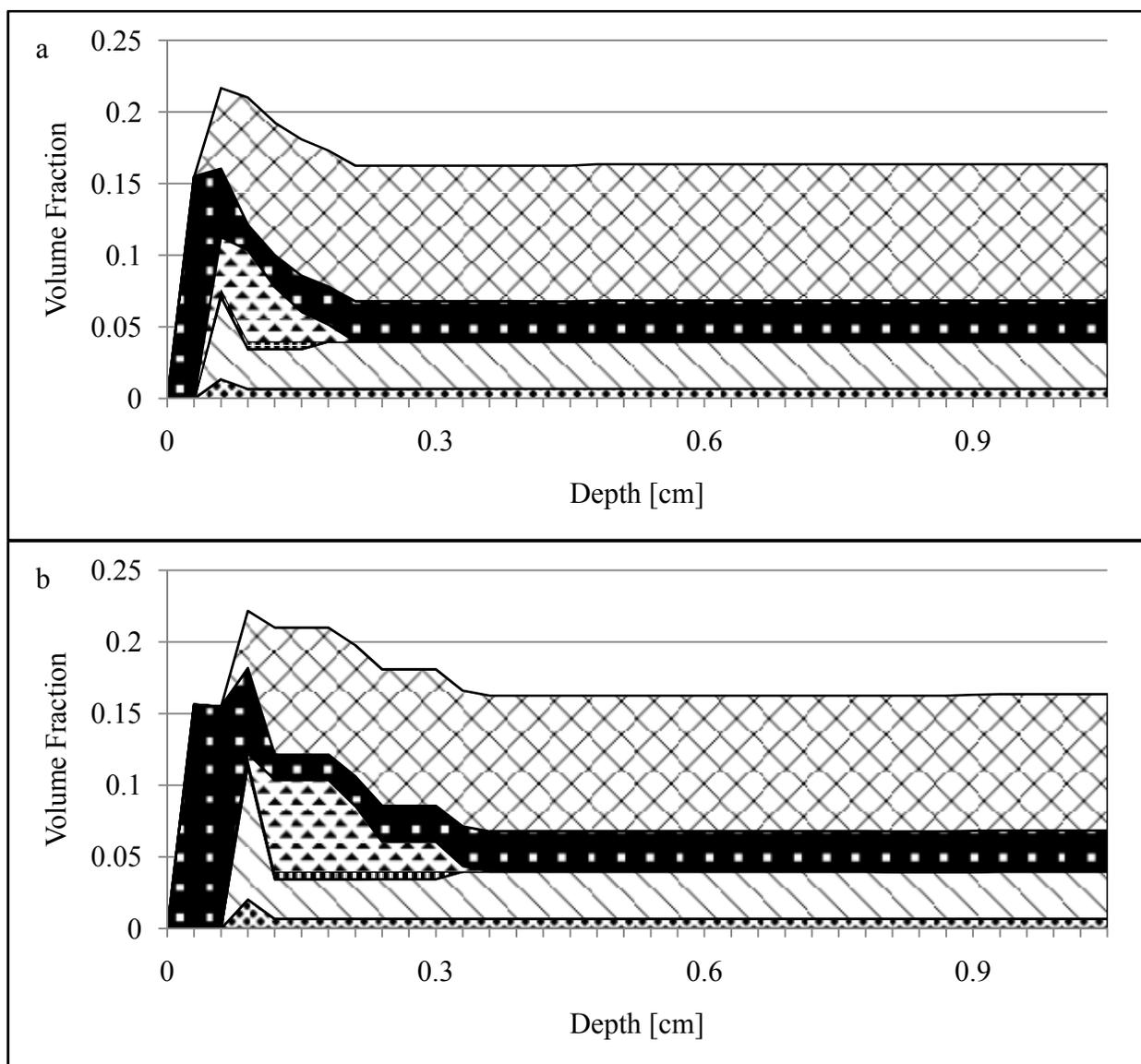
Fig. 2: Contributions of individual solid species to total mineral volume at a) 6 weeks and b) 24 weeks of storage in a 5% CO2 (g) atmosphere at 70% saturation. The solid phases present are: portlandite (hatch), calcite (white squares), tricarboaluminate (black triangles), Fe-ettringite (vertical stripes), ettringite (diagonal lines), C-S-H (black circles).

A comparison of net porosity change after 24 weeks of conditioning is shown in Figure 3. Porosity is increased nearly threefold in the first cell for the case of DI water leaching but the zone of increased porosity only extends to a depth of about 9mm. Similarly, after 24 weeks of $CO_2(g)$ exposure, the first cell of the specimen has increased in porosity due to the dissolution of several of the primary phases. Beyond the dissolution region near the specimen surface, precipitation of calcite and tricarboaluminate filled about 50% of the initial porosity, and this region of porosity filling extends to a depth of about 33 mm. The corresponding tortuosities calculated from Eq. (4) are illustrated in Figure 3 (b). Despite having a maximum net porosity change only one fourth of that of the DI water leaching, the porosity filling of $CO_2(g)$ exposure

results in a maximum net tortuosity increase of about 33% as compared to about 67% decrease for DI water leaching. Thus, the relative sensitivity of Eq. (4) to porosity filling is demonstrated.
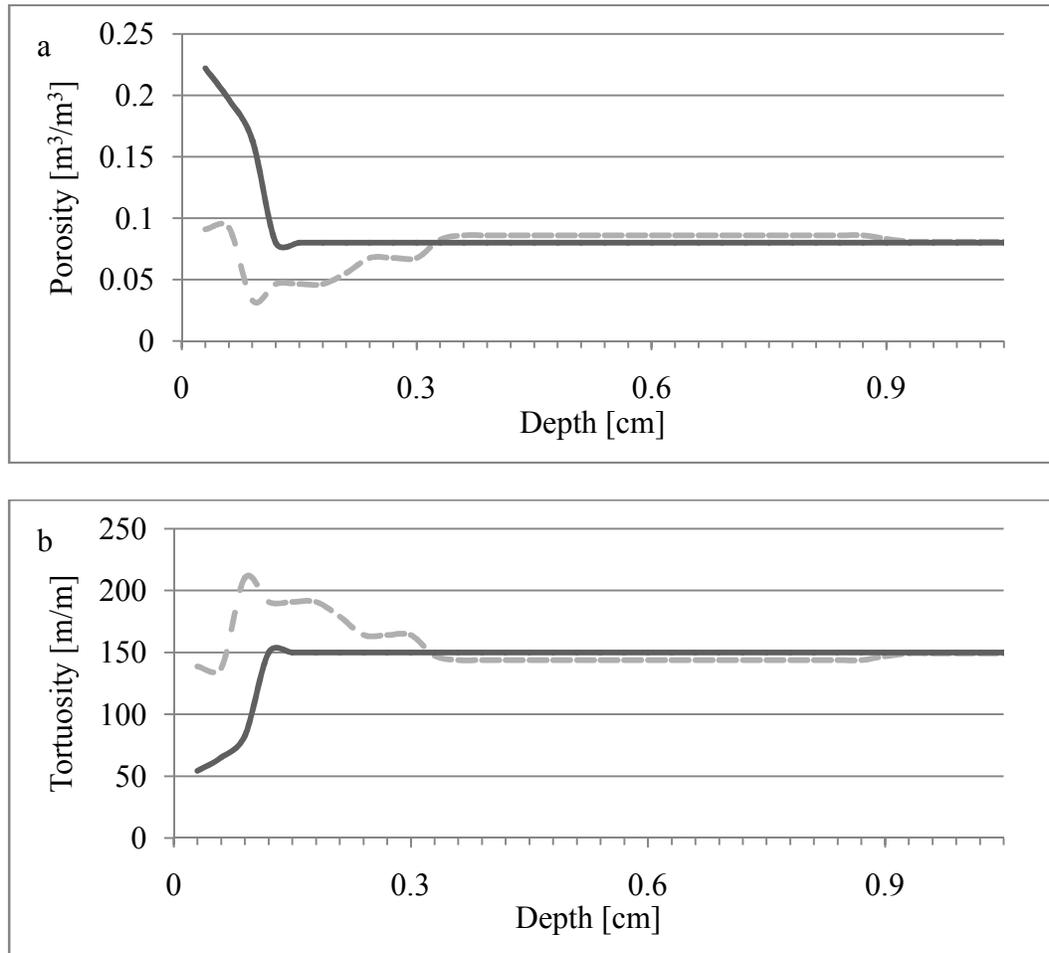

Figure 3: Simulated porosity (a) and tortuosity (b) profiles after 24 weeks of conditioning for the cases of deionized water leaching (solid line) and storage in a 5% CO_2(g) atmosphere (dashed line).

In order to demonstrate the influence of porosity alteration on constituent migration, the intrusion of a conservative, non-reactive tracer into fully saturated, porosity-altered specimens was simulated. In the simulation, a finite volume of the tracer was exposed to the specimen boundary at a concentration of 1 [mol/L]. Simulation was executed for 28 days during which no further chemical reactions were allowed to occur. The resulting concentration profiles are shown in Figure 4. Comparison of the baseline (no porosity change) concentration profile to the DI water-leached profile reveals a significant acceleration in the tracer diffusion front in as little as 28 days. Conversely, the mineral precipitation induced by gaseous carbonation served to deter the progression of the tracer front after the front had reached the low porosity zone beginning at depth of 0.09 cm. Prior to reaching this depth, the tracer concentration front is actually accelerated compared to the baseline due to the lowered porosity in this zone.
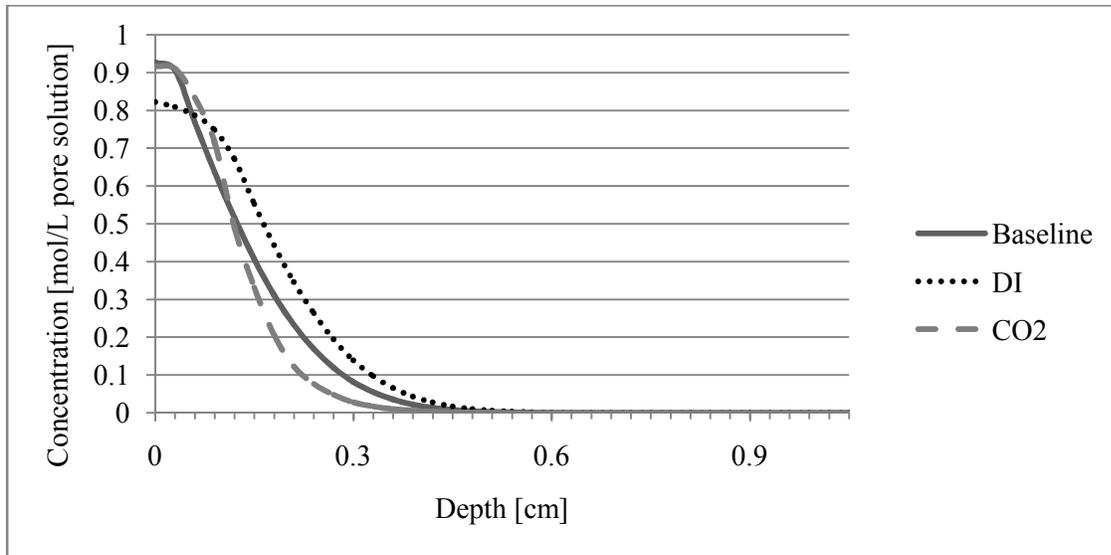
Figure 4: Tracer concentration profiles from simulations of diffusion into fully saturated specimens with no porosity change (Baseline), porosity change due to DI water leaching (DI), and porosity change due to gaseous CO_2 carbonation (CO2).

CONCLUSIONS

Net porosity change of cementitious materials was demonstrated to depend on the dissolution and precipitation of multiple solid species. The ingress of a trace constituent was shown to be significantly dependent upon the porosity changes induced through deionized water leaching and gaseous phase carbonation. In spite of an increased leaching of calcium in the surficial layers of the material, gaseous phase carbonation deterred the ingress of a trace constituent. As expected, deionized water leaching of the material served to accelerate the progression of the tracer intrusion front. In scenarios involving coincident porosity filling and opening, whether the aging phenomena involved are deemed favorable or unfavorable may vary greatly depending on the initial chemistry of the material, the concentrations of intruding reacting species, and the rate and frequency of intrusion. Thus, modeling of the coupled chemical and physical phenomena encompassed in an holistic approach to environmental aging of cementitious materials necessitates extensive experimental validation.

ACKNOWLEDGMENTS

REFERENCES

1. D.S. Kosson, et al., "An Integrated Framework for Evaluating Leaching in Waste Management and Utilization of Secondary Materials," *Environmental Engineering Science*, vol. 19, no. 3, 2002, pp. 159-204; DOI doi:10.1089/109287502760079188.
2. T. Matschei, et al., "Thermodynamic properties of Portland cement hydrates in the system CaO-Al2O3-SiO2-CaSO4-CaCO3-H2O," *Cement and Concrete Research*, vol. 37, no. 10, 2007, pp. 1379-1410.
3. J. Marchand, et al., "Ion transport mechanisms in cement-based materials," *Materials Science of Concrete*, vol. V, 1998, pp. 307–400.
4. E.J. Garboczi and D.P. Bentz, "Computer simulation of the diffusivity of cement-based materials," *Journal of Materials Science*, vol. 27, no. 8, 1992, pp. 2083-2092.
5. M. Mainguy, et al., "Modelling of leaching in pure cement paste and mortar," *Cement and Concrete Research*, vol. 30, no. 1, 2000, pp. 83-90.
6. K. Haga, et al., "Effects of porosity on leaching of Ca from hardened ordinary Portland cement paste," *Cement and Concrete Research*, vol. 35, no. 9, 2005, pp. 1764-1775.
7. E. Samson and J. Marchand, "Modeling the transport of ions in unsaturated cement-based materials," *Computers & Structures*, vol. 85, no. 23-24, 2007, pp. 1740-1756.